transplant candidates with a non-HCC diagnosis.[44] They found that the dropout risk of HCC patients was predicted by the MELD score, HCC size, HCC number and AFP, and they calculated the dropout equivalent MELD (deMELD) points that express similar risks of dropout between HCC and non-HCC patients and allow for the management of both groups on a common waiting list.[44] The deMELD equation was obtained as follows:

$$\text{deMELD} = -25 + 0.1 \times \text{age} + 1.6 \times \text{MELD} + 1.6 \times \text{tumor size} + 1.3 \times \log(\text{AFP}),$$

+6 if tumor number ≥2, +0 if diagnosis = HCV, −1 if diagnosis = hepatitis B virus, +3 if diagnosis = alcohol, +3 if diagnosis = non-alcoholic steatohepatitis, +1 if diagnosis = hemochromatosis, +1 if diagnosis = other.

AFP LEVELS IN SORAFENIB-TREATED HCC PATIENTS

SORAFENIB IS AN antiangiogenic agent used to treat advanced HCC.[45,46] Sorafenib sometimes induces disappearance of contrast enhancement of HCC at the arterial phase, but rarely induces HCC shrinkage. Therefore, it is difficult to evaluate the antitumor effect of sorafenib or to predict its survival effect by imaging-based Response Evaluation Criteria in Solid Tumors (RECIST). Personeni *et al.* investigated the prognostic usefulness of a decrease in serum AFP levels and compared it to RECIST in 82 HCC patients treated with sorafenib.[47] AFP response (≥20% decrease in AFP during 8 weeks of treatment) rather than the radiological outcomes evaluated by RECIST was a significant prognostic factor for survival in multivariate analysis. The authors concluded that the assessment of AFP response was superior to RECIST in determining the response to sorafenib treatment.[47] Similarly, Yau *et al.* reported that decreased AFP levels (≥20% of the baseline level after 6 weeks of sorafenib) were significantly associated with progression-free survival both in 41 exploration patients and 53 validation patients.[48] When Kuzuya *et al.* evaluated the relationships between antitumor response based on imaging studies and early changes (2 and 4 weeks after starting sorafenib therapy) in AFP and DCP levels, they found that a significant early decrease in AFP levels was observed in the partial response and stable disease groups, while DCP levels increased despite therapeutic efficacy.[49] The authors speculated that the ischemic change of HCC cells may result in the elevation of DCP level, and concluded that AFP levels rather than DCP levels are useful for predicting antitumor responses during sorafenib therapy. In addition, the retrospective analysis of 66 patients treated with sorafenib revealed that assessment of overall survival by a change in AFP ratio of 1 or less at 8 weeks was better than that of more than 1 at 8 weeks ($P = 0.002$), but DCP ratio was not useful for assessment of overall survival.[50]

HS-AFP-L3

LENS CULINARIS AGGLUTININ-REACTIVE AFP, a fucosylated fraction of AFP, is a highly specific marker for HCC compared with AFP, and its elevation links to poor prognosis.[51] However, the advantage of AFP-L3 measured by conventional method had been limited due to its low sensitivity, especially in patients with total AFP below 20 ng/mL. To resolve this issue, a hs-AFP-L3 assay has been recently developed. There are several studies supporting the clinical utility of a newly developed hs-AFP-L3 assay in patients with low total AFP levels.[52–56] Toyoda *et al.* reported that sensitivity and specificity of hs-AFP-L3 for HCC in patients with total AFP below 20 ng/mL was 25–50% and more than 85%, respectively, at the cut-off level between 5% and 7%.[57] These results suggest that hs-AFP-L3 is 5–10-times more sensitive than conventional AFP-L3, maintaining high specificity. They proposed that hs-AFP-L3 elevation in patients with total AFP level below 20 ng/mL indicates poor prognosis of HCC and predicts detection of HCC in high-risk patients under surveillance. Thus it is possible that hs-AFP-L3 is a useful biomarker for detection and management of HCC, especially in patients with low total AFP.

REFERENCES

1 Nakata K, Motomura M, Nakabayashi H, Ido A, Tamaoki T. A possible mechanism of inverse developmental regulation of alpha-fetoprotein and albumin genes. Studies with epidermal growth factor and phorbol ester. *J Biol Chem* 1992; **267**: 1331–4.
2 Tsutsumi T, Ido A, Nakao K *et al.* Reciprocal regulation of alpha-fetoprotein and albumin gene expression by butyrate in human hepatoma cells. *Gastroenterology* 1994; **107**: 499–504.
3 Hu KQ, Kyulo NL, Lim N, Elhazin B, Hillebrand DJ, Bock T. Clinical significance of elevated alpha-fetoprotein (AFP) in patients with chronic hepatitis C, but not hepatocellular carcinoma. *Am J Gastroenterol* 2004; **99**: 860–5.
4 Schiødt FV, Ostapowicz G, Murray N *et al.* Alpha-fetoprotein and prognosis in acute liver failure. *Liver Transpl* 2006; **12**: 1776–81.
5 Sherman M. The resurrection of alphafetoprotein. *J Hepatol* 2010; **52**: 939–40.

6 Riaz A, Ryu RK, Kulik LM *et al.* Alpha-fetoprotein response after locoregional therapy for hepatocellular carcinoma: oncologic marker of radiologic response, progression, and survival. *J Clin Oncol* 2009; **27**: 5734–42.
7 Li HM, Ikeda H, Nakabayashi H, Nishi S, Sakai M. Identification of CCAAT enhancer binding protein alpha binding sites on the human alpha-fetoprotein gene. *Gene* 2007; **389**: 128–35.
8 Nakabayashi H, Koyama Y, Suzuki H *et al.* Functional mapping of tissue-specific elements of the human alpha-fetoprotein gene enhancer. *Biochem Biophys Res Commun* 2004; **318**: 773–85.
9 Peterson ML, Ma C, Spear BT. Zhx2 and Zbtb20: novel regulators of postnatal alpha-fetoprotein repression and their potential role in gene reactivation during liver cancer. *Semin Cancer Biol* 2011; **21**: 21–7.
10 Kajiyama Y, Tian J, Locker J. Characterization of distant enhancers and promoters in the albumin-alpha-fetoprotein locus during active and silenced expression. *J Biol Chem* 2006; **281**: 30122–31.
11 Jin L, Long L, Green MA, Spear BT. The alpha-fetoprotein enhancer region activates the albumin and alpha-fetoprotein promoters during liver development. *Dev Biol* 2009; **336**: 294–300.
12 Perincheri S, Dingle RW, Peterson ML, Spear BT. Hereditary persistence of alpha-fetoprotein and H19 expression in liver of BALB/cJ mice is due to aretrovirus insertion in the Zhx2 gene. *Proc Natl Acad Sci U S A* 2005; **102**: 396–401.
13 Xie Z, Zhang H, Tsai W *et al.* Zinc finger protein ZBTB20 is a key repressor of alpha-fetoprotein gene transcription in liver. *Proc Natl Acad Sci U S A* 2008; **105**: 10859–64.
14 Shen H, Luan F, Liu H *et al.* ZHX2 is a repressor of alpha-fetoprotein expression in human hepatoma cell lines. *J Cell Mol Med* 2008; **12**: 2772–80.
15 Lv Z, Zhang M, Bi J, Xu F, Hu S, Wen J. Promoter hypermethylation of a novel gene, ZHX2, in hepatocellular carcinoma. *Am J Clin Pathol* 2006; **125**: 740–6.
16 Morford LA, Davis C, Jin L, Dobierzewska A, Peterson ML, Spear BT. The oncofetal gene glypican 3 is regulated in the postnatal liver by zinc fingers and homeoboxes 2 and in the regenerating liver by alpha-fetoprotein regulator 2. *Hepatology* 2007; **46**: 1541–7.
17 Yue X, Zhang Z, Liang X *et al.* Zinc fingers and homeoboxes 2 inhibits hepatocellular carcinomacell proliferation and represses expression of Cyclins A and E. *Gastroenterology* 2012; **142**: 1559–70.
18 Kojima K, Takata A, Vadnais C *et al.* MicroRNA122 is a key regulator of α-fetoprotein expression and influences the aggressiveness of hepatocellular carcinoma. *Nat Commun* 2011; **2**: 338.
19 Richardson P, Duan Z, Kramer J, Davila JA, Tyson GL, El-Serag HB. Determinants of serum alpha-fetoprotein levels in hepatitis C-infected patients. *Clin Gastroenterol Hepatol* 2012; **10**: 428–33.
20 Tateyama M, Yatsuhashi H, Taura N *et al.* Alpha-fetoprotein above normal levels as a risk factor for the development of hepatocellular carcinoma in patients infected with hepatitis Cvirus. *J Gastroenterol* 2011; **46**: 92–100.
21 Abdoul H, Mallet V, Pol S, Fontanet A. Serum alpha-fetoprotein predicts treatment outcome in chronic hepatitis C patients regardless of HCV genotype. *PLoS ONE* 2008; **3**: e2391.
22 Chen TM, Huang PT, Tsai MH *et al.* Predictors of alpha-fetoprotein elevation in patients with chronic hepatitis C, but not hepatocellular carcinoma, and its normalization after pegylatedinterferon alfa 2a-ribavirin combination therapy. *J Gastroenterol Hepatol* 2007; **22**: 669–75.
23 Murashima S, Tanaka M, Haramaki M *et al.* A decrease in AFP level related to administration of interferon in patients with chronic hepatitis C and a high level of AFP. *Dig Dis Sci* 2006; **51**: 808–12.
24 Nomura H, Kashiwagi Y, Hirano R *et al.* Efficacy of low dose long-term interferon monotherapy in aged patients with chronic hepatitis C genotype 1 and its relation to alpha-fetoprotein: a pilot study. *Hepatol Res* 2007; **37**: 490–7.
25 Kajiwara E, Ooho A, Yamashita N. Effectiveness of biweekly low-dosage peginterferon treatment on the improvement of serum alanine aminotransferase and α-fetoprotein levels. *Hepatol Res* 2012; **42**: 254–63.
26 Tamura Y, Yamagiwa S, Aoki Y *et al.* Niigata Liver Disease Study Group. Serum alpha-fetoprotein levels during and after interferon therapy and the development of hepatocellular carcinoma in patients with chronic hepatitis C. *Dig Dis Sci* 2009; **54**: 2530–7.
27 Osaki Y, Ueda Y, Marusawa H *et al.* Decrease in alpha-fetoprotein levels predicts reduced incidence of hepatocellular carcinoma in patients with hepatitis C virus infection receiving interferon therapy: a single center study. *J Gastroenterol* 2012; **47**: 444–51.
28 Akuta N, Suzuki F, Kawamura Y *et al.* Substitution of amino acid 70 in the hepatitis C virus core region of genotype 1b is an important predictor of elevated alpha-fetoprotein in patients without hepatocellular carcinoma. *J Med Virol* 2008; **80**: 1354–62.
29 Akuta N, Suzuki F, Kawamura Y *et al.* Predictive factors of early and sustained responses to peginterferon plus ribavirin combination therapy in Japanese patients infected with hepatitis C virus genotype 1b: amino acid substitutions in the core region and low-density lipoprotein cholesterol levels. *J Hepatol* 2007; **46**: 403–10.
30 Akuta N, Suzuki F, Kawamura Y *et al.* Amino acid substitutions in the hepatitis C virus core region are the important predictor of hepatocarcinogenesis. *Hepatology* 2007; **46**: 1357–64.
31 Akuta N, Suzuki F, Hirakawa M *et al.* Amino acid substitutions in hepatitis C virus core region predict hepatocarcinogenesis following eradication of HCV RNA by antiviral therapy. *J Med Virol* 2011; **83**: 1016–22.

32 Hakeem AR, Young RS, Marangoni G, Lodge JP, Prasad KR. Systematic review: the prognostic role of alpha-fetoprotein following liver transplant for hepatocellular carcinoma. *Aliment Pharmacol Ther* 2012; **35**: 987–99.

33 Duvoux C, Roudot-Thoraval F, Decaens T *et al.* Liver Transplantation French Study Group. Liver transplantation for hepatocellular carcinoma: a model including α-fetoprotein improves the performance of Milan criteria. *Gastroenterology* 2012; **143**: 986–94.

34 Muscari F, Guinard JP, Kamar N, Peron JM, Otal P, Suc B. Impact of preoperative α-fetoprotein level on disease-free survival after liver transplantation for hepatocellular carcinoma. *World J Surg* 2012; **36**: 1824–31.

35 Xu X, Ke QH, Shao ZX *et al.* The value of serum alpha-fetoprotein in predicting tumor recurrence after liver transplantation for hepatocellular carcinoma. *Dig Dis Sci* 2009; **54**: 385–8.

36 Cescon M, Ravaioli M, Grazi GL *et al.* Prognostic factors for tumor recurrence after a 12-year, single-center experience of liver transplantations in patients with hepatocellular carcinoma. *J Transplant* 2010; doi: 10.1155/2010/904152.

37 Han K, Tzimas GN, Barkun JS *et al.* Preoperative alpha-fetoprotein slope is predictive of hepatocellular carcinoma recurrence after liver transplantation. *Can J Gastroenterol* 2007; **21**: 39–45.

38 Mailey B, Artinyan A, Khalili J *et al.* Evaluation of absolute serum α-fetoprotein levels in liver transplant for hepatocellular cancer. *Arch Surg* 2011; **146**: 26–33.

39 Todo S, Furukawa H, Tada M, Japanese Liver Transplantation Study Group. Extending indication: role of living donor liver transplantation for hepatocellular carcinoma. *Liver Transpl* 2007; **13**: S48–54.

40 Wang ZX, Song SH, Teng F *et al.* A single-center retrospective analysis of liver transplantation on 255 patients with hepatocellular carcinoma. *Clin Transplant* 2010; **24**: 752–7.

41 Fujiki M, Takada Y, Ogura Y *et al.* Significance of des-gamma-carboxy prothrombin in selection criteria for living donor liver transplantation for hepatocellular carcinoma. *Am J Transplant* 2009; **9**: 2362–71.

42 Yao FY, Kerlan RK Jr, Hirose R *et al.* Excellent outcome following down-staging of hepatocellular carcinoma prior to liver transplantation: an intention-to-treat analysis. *Hepatology* 2008; **48**: 819–27.

43 Merani S, Majno P, Kneteman NM *et al.* The impact of waiting list alpha-fetoprotein changes on the outcome of liver transplant for hepatocellular carcinoma. *J Hepatol* 2011; **55**: 814–9.

44 Toso C, Dupuis-Lozeron E, Majno P *et al.* A model for dropout assessment of candidates with or without hepatocellular carcinoma on a common liver transplant waiting list. *Hepatology* 2012; **56**: 149–56.

45 Llovet JM, Ricci S, Mazzaferro V *et al.* SHARP Investigators Study Group. Sorafenib in advanced hepatocellular carcinoma. *N Engl J Med* 2008; **359**: 378–90.

46 Cheng AL, Kang YK, Chen Z *et al.* Efficacy and safety of sorafenib in patients in the Asia-Pacific region with advanced hepatocellular carcinoma: a phase III randomised, double-blind, placebo-controlled trial. *Lancet Oncol* 2009; **10**: 25–34.

47 Personeni N, Bozzarelli S, Pressiani T *et al.* Usefulness of alpha-fetoprotein response in patients treated with sorafenib for advanced hepatocellular carcinoma. *J Hepatol* 2012; **57**: 101–7.

48 Yau T, Yao TJ, Chan P *et al.* The significance of early alpha-fetoprotein level changes in predicting clinical and survival benefits in advanced hepatocellular carcinoma patients receiving sorafenib. *Oncologist* 2011; **16**: 1270–9.

49 Kuzuya T, Asahina Y, Tsuchiya K *et al.* Early decrease in α-fetoprotein, but not des-γ-carboxy prothrombin, predicts sorafenib efficacy in patients with advanced hepatocellular carcinoma. *Oncology* 2011; **81**: 251–8.

50 Kawaoka T, Aikata H, Murakami E *et al.* Evaluation of the mRECIST and α-fetoprotein ratio for stratification of the prognosis of advanced hepatocellular carcinoma patients treated with Sorafenib. *Oncology* 2012; **83**: 192–200.

51 Yamashita F, Tanaka M, Satomura S, Tanikawa K. Prognostic significance of Lens culinaris agglutinin A-reactive alpha-fetoprotein in small hepatocellular carcinomas. *Gastroenterology* 1996; **111**: 996–1001.

52 Tamura Y, Igarashi M, Kawai H, Suda T, Satomura S, Aoyagi Y. Clinical advantage of highly sensitive on-chip immunoassay for fucosylated fraction of alpha-fetoprotein in patients with hepatocellular carcinoma. *Dig Dis Sci* 2010; **55**: 3576–83.

53 Hanaoka T, Sato S, Tobita H *et al.* Clinical significance of the highly sensitive fucosylated fraction of α-fetoprotein in patients with chronic liver disease. *J Gastroenterol Hepatol* 2011; **26**: 739–44.

54 Toyoda H, Kumada T, Tada T *et al.* Clinical utility of highly sensitive Lens culinaris agglutinin-reactive alpha-fetoprotein in hepatocellular carcinoma patients with alpha-fetoprotein <20 ng/mL. *Cancer Sci* 2011; **102**: 1025–31.

55 Nouso K, Kobayashi Y, Nakamura S *et al.* Prognostic importance of fucosylated alpha-fetoprotein in hepatocellular carcinoma patients with low alpha-fetoprotein. *J Gastroenterol Hepatol* 2011; **26**: 1195–200.

56 Kobayashi M, Hosaka T, Ikeda K *et al.* Highly sensitive AFP-L3% assay is useful for predicting recurrence of hepatocellular carcinoma after curative treatment pre- and post-operatively. *Hepatol Res* 2011; **41**: 1036–45.

57 Toyoda H, Kumada T, Tada T. Highly sensitive Lens culinaris agglutinin-reactive α-fetoprotein: a new tool for the management of hepatocellular carcinoma. *Oncology* 2011; **81**: 61–5.

Journal of Controlled Release 166 (2013) 203–210

Contents lists available at SciVerse ScienceDirect

Journal of Controlled Release

journal homepage: www.elsevier.com/locate/jconrel

Injectable hyaluronic acid-tyramine hydrogels incorporating interferon-α2a for liver cancer therapy

Keming Xu [a], Fan Lee [a], Shu Jun Gao [a], Joo Eun Chung [a], Hirohisa Yano [a,b], Motoichi Kurisawa [a,*]

[a] Institute of Bioengineering and Nanotechnology, 31 Biopolis Way, The Nanos, 138669, Singapore
[b] Department of Pathology, Kurume University School of Medicine, Kurume, Fukuoka, 830-0011, Japan

ARTICLE INFO

Article history:
Received 16 November 2012
Accepted 5 January 2013
Available online 14 January 2013

Keywords:
Hydrogel
Injectable
Protein delivery
Hyaluronic acid
Interferon

ABSTRACT

We report an injectable hydrogel system that incorporates interferon-α2a (IFN-α2a) for liver cancer therapy. IFN-α2a was incorporated in hydrogels composed of hyaluronic acid-tyramine (HA-Tyr) conjugates through the oxidative coupling of Tyr moieties with hydrogen peroxide (H_2O_2) and horseradish peroxidase (HRP). IFN-α2a-incorporated HA-Tyr hydrogels of varying stiffness were formed by changing the H_2O_2 concentration. The incorporation of IFN-α2a did not affect the rheological properties of the hydrogels. The activity of IFN-α2a was furthermore well-maintained in the hydrogels with lower stiffness. Through the caspase-3/7 pathway *in vitro*, IFN-α2a released from HA-Tyr hydrogels inhibited the proliferation of liver cancer cells and induced apoptosis. In the study of the pharmacokinetics, a higher concentration of IFN-α2a was shown in the plasma of mice treated with IFN-α2a-incorporated hydrogels after 4 h post injection, with a much higher amount of IFN-α2a delivered at the tumor tissue comparing to that of injecting an IFN-α2a solution. The tumor regression study revealed that IFN-α2a-incorporated HA-Tyr hydrogels effectively inhibited tumor growth, while the injection of an IFN-α2a solution did not demonstrate antitumor efficacy. Histological studies confirmed that tumor tissues in mice treated with IFN-α2a-incorporated HA-Tyr hydrogels showed lower cell density, with more apoptotic and less proliferating cells compared with tissues treated with an IFN-α2a solution. In addition, the IFN-α2a-incorporated hydrogel treatment greatly inhibited the angiogenesis of tumor tissues.

1. Introduction

Therapeutic proteins are a major class of pharmaceuticals. As of 2010, there had been 200 protein based products approved for therapeutic applications with more than 600 under development [1]. Protein therapeutics consist of monoclonal antibodies and vaccines, as well as hormones, growth factors, cytokines, enzymes, etc. They can provide treatments for a variety of diseases, ranging from microbial infection [2] to autoimmune diseases [3] and cancer [4]. One of the greatest advantages of using protein therapeutics is the capacity to produce high affinity and specificity antibodies to virtually any target of interest, through transgenic mice and/or phage display technologies [5]. Yet many of these protein drugs, with the exception of whole antibodies and Fc-fusion proteins [6], possess a rather short terminal half-life in the range of minutes to hours. These proteins usually undergo rapid clearance by peripheral blood-mediated proteolysis, renal and hepatic elimination, as well as elimination by receptor-mediated endocytosis [6]. In order to maintain an effective concentration of protein drugs during therapy, frequent infusions are applied that often lead to various side-effects and discomfort for patients [7]. Thus, a drug delivery system for the prolonged release of protein therapeutics is highly desirable.

The use of hydrogels as depots for prolonged drug release has been extensively studied. As hydrogels imbibe large amounts of water, they can provide an aqueous environment for protein therapeutics and prevent their denaturation [8]. An injectable hydrogel system is particularly useful in drug delivery as surgery is not required for implantation. Recently, an enzymatic crosslinking strategy has attracted intensive attention in the area of drug delivery and regenerative medicine [9,10]. We have previously reported an injectable and biodegradable hydrogel system composed of hyaluronic acid-tyramine conjugates (HA-Tyr) [11,12]. The hydrogels were formed through the oxidative coupling reaction of the Tyr moieties, catalyzed by hydrogen peroxide (H_2O_2) and horseradish peroxidase (HRP).

The advantage of the enzymatically-crosslinked HA-Tyr hydrogel system is the independent tuning of hydrogel stiffness and gelation rate [13]. The stiffness of HA-Tyr hydrogels could be controlled by the concentration of H_2O_2 while the gelation rate was tuned by the concentration of HRP. It was previously demonstrated that model proteins, such as lysozyme and α-amylase, could be incorporated and subsequently released from HA-Tyr hydrogels. Moreover, the protein release profile and the activity of released proteins were

* Corresponding author. Tel.: +65 6824 7139; fax: +65 6478 9083.
E-mail address: mkurisawa@ibn.a-star.edu.sg (M. Kurisawa).

0168-3659/$ – see front matter © 2013 Elsevier B.V. All rights reserved.
http://dx.doi.org/10.1016/j.jconrel.2013.01.008

shown to depend on the stiffness of the hydrogel as well as the isoelectric point of the protein [14]. Other *in situ* forming HA-based hydrogel systems, such as thiolated HA which crosslink *via* poly(ethylene glycol) diacrylate (PEGDA) by addition reaction [15,16] or furan-modified HA which crosslink *via* dimaleimide poly(ethylene glycol) by Diels–Alder reaction [17], require extensive modifications to HA with the degree of substitution between 40 to 60%. By comparison, the degree of substitution of HA-Tyr is relatively low (4–6%) and yet hydrogels can be formed rapidly by the enzyme-mediated oxidative reaction. Indeed, it was demonstrated that HA-Tyr hydrogels with a gel point of 1–2 min could effectively incorporate proteins within the gel matrix and thus prevent undesired leakage of the gel precursors and proteins into the surrounding tissue.

From these perspectives, we consider that the design of an injectable hydrogel system that incorporated protein therapeutics would be important for the treatment of diseases. Herein, the anticancer effect of IFN-α2a-incorporated HA-Tyr hydrogels was explored *in vitro* and *in vivo* and compared to the effect of IFN-α2a solution. IFN-α2a, one of the IFN analogues, is a class of cytokines with various functions, the most well-known of which is its anti-viral activity [18,19]. In recent years, there are increasing numbers of reports that demonstrate IFN inhibits the proliferation and induces apoptosis of cancer cells in hepatocellular carcinoma [20,21]. In this study, we first prepared IFN-α2a-incorporated HA-Tyr hydrogels with varying stiffness and studied the release of the protein from hydrogels *in vitro*. After that, we examined the activity of proteins incorporated in the hydrogels using cells with subgenomic Hepatitis C virus (HCV) replicon. Then, we confirmed the inhibition of proliferation and induction of apoptosis of human liver cancer cells HAK-1B with IFN-incorporated HA-Tyr hydrogels *in vitro*. In an animal experiment, we studied the pharmacokinetics of the protein drug in the plasma of hydrogel-treated mice and also the amount of IFN-α2a delivered at the tumor tissue. Finally, we evaluated the efficacy of IFN-α2a-incorporated HA-Tyr hydrogels in tumor regression with a HAK-1B-xenografted nude mice model. The histology and immunohistochemistry of tumor tissues were also characterized on mice treated with PBS, IFN-α2a alone or IFN-α2a-incorporated hydrogels.

2. Materials and methods

2.1. Materials and cell culture

Sodium hyaluronate (HA) (MW = 90 kDa, density = 1.05 g/cm^3) was kindly donated by JNC Corporation (Tokyo, Japan). Hyaluronidase (439 units/mg) from bovine testes was purchased from Sigma-Aldrich (Singapore). Horseradish peroxidase (HRP, 100 units/mg) was obtained from Wako Pure Chemical Industries (Osaka, Japan). Interferon α2a (IFN-α2a, 1×10^8 IU/mg protein) was purchased from Santa Cruz (CA, USA). VeriKine™ Human Interferon-Alpha ELISA kit was purchased from PBL Interferon Source (NJ, USA). Luciferase assay system and Apo-ONE® homogeneous caspase-3/7 assay kit were purchased from Promega (Singapore). AlarmarBlue assay kit, Alexa Fluor® 488 annexin V/Dead cell apoptosis kit for flow cytometry and Image-iT™ live red caspase detection kit were purchased from Life Technologies (Singapore). Bicinchoninic acid (BCA) protein assay kit was purchased from Pierce (Singapore).

The human hepatic cancer cell line (HAK-1B) was obtained from Prof. Hirohisa Yano, Kurume University, Japan and was grown in DMEM media with 2.5% fetal bovine serum (GIBCO, Singapore) [22]. Huh-7 cells containing subgenomic HCV replicon I_{389}luc-ubi-neo/NS3-3/5.1 with adaptive mutation (E1202G, T1280I, K1846T) were obtained from Prof. Ralf Bartenschlager, University of Heidelberg, Germany, and were grown in DMEM media with 10% fetal bovine serum, 1 mM non-essential amino acid and 500 μg/ml G418 (Geneticin, Merck) [23,24]. All cells were cultured in a humidified incubator at 37 °C, 5% CO_2.

2.2. Synthesis of IFN-α2a-incorporated HA-Tyr hydrogels and rheological measurements

Hyaluronic acid-tyramine (HA-Tyr) conjugates were synthesized and the rheological measurement was performed as previously described [13]. Briefly, samples were prepared by adding 65 μl of IFN-α2a dissolved in PBS to 175 μl of HA-Tyr solution (2.5 wt.%), followed by addition of 5 μl each of HRP (6.2 units/ml) and hydrogen peroxide (H_2O_2) in varying concentrations. The final concentrations of HA-Tyr, IFN-α2a, and HRP were 1.75 wt.%, 2.5×10^5 IU/ml and 0.124 units/ml, respectively. The mixture was immediately vortexed and 210 μl was applied to the bottom plate of the rheometer. Rheological measurement was allowed to proceed until the sample's storage modulus (G') reached a plateau.

2.3. Crosslinking density and mesh size of IFN-α2a-incorporated HA-Tyr hydrogels

The mesh size (ξ) and crosslinking density (ν_e) of the HA-Tyr hydrogels were determined by previously described methods [25]. Briefly, 200 μl of HA-Tyr hydrogels with or without IFN-α2a were prepared and swelled in 20 ml of PBS for 24 h. The swollen hydrogels were weighed (swollen weight as M_s) and lyophilized. Then, the dried weights were determined (dried weight as M_d) and the mass swelling ratio (Q_M) was calculated by dividing M_s with M_d. The volumetric swelling ratio (Q_V), effective crosslink density (ξ) and mesh size (ν_e) were then calculated as described in the literature [25].

2.4. Release of IFN-α2a from HA-Tyr hydrogels in vitro

HA-Tyr hydrogels that incorporated 2.5×10^5 IU/ml of IFN-α2a were prepared by mixing 778 μl of HA-Tyr conjugate (2.25 wt.%) with 100 μl of IFN-α2a solution (2.5×10^6 IU/ml) and 112 μl of PBS. Five microliters each of HRP and H_2O_2 (final concentrations of HRP: 0.124 units/ml and H_2O_2: 437 μM or 728 μM) were then added. The solution was gently mixed by pipetting and then injected between two parallel glass plates clamped 1.5 mm apart. Gelation was allowed to proceed at 37 °C for 2 h. Round gel disks, 1.6 cm in diameter, were then cut from the hydrogel slab using a circular mold. Each disk was placed in a plastic net and immersed in 20 ml of buffer solution (PBS with 0.5% BSA). At selected time points, 200 μl of the media was withdrawn and replaced with an equal volume of fresh buffer solution to maintain a constant total volume. The collected samples were stored in LoBind tubes (Eppendorf, Germany) at 4 °C until measurement. Protein concentrations were determined using a VeriKine™ Human Interferon-Alpha ELISA kit.

2.5. Activity of IFN-α2a incorporated in HA-Tyr hydrogels

HA-Tyr hydrogels that incorporated 2.5×10^5 IU/ml of IFN-α2a were prepared as mentioned above. The complete degradation of the hydrogel was achieved after overnight incubation with 250 U/ml hyaluronidase at 37 °C. The solution mixture of degraded hydrogels was diluted to 2 and 4 pg/ml IFN-α2a with DMEM media and a Huh-7-based assay was performed on them. Typically, 200,000 of Huh-7 cells were seeded on each well of 6-well plates in DMEM with G418. After 24 h, the media was aspirated and the cells were treated with DMEM media (without G418) mixed with the solution of degraded hydrogels, or 1000 IU/ml of IFN-α2a. After 72 h, the cell lysate was collected and a luciferase assay (Promega, Singapore) was carried out to measure the value of relative luminescence unit (RLU) for each sample. The inhibitory activity of IFN-α2a was calculated by the following equation:

$$\text{Inhibition } (\%) = \frac{\text{Log}_{10}(\text{NC}) - \text{Log}_{10}(S_n)}{\text{Log}_{10}(\text{NC}) - \text{Log}_{10}(\text{PC})} \times 100$$

where PC is the value of RLU after incubation with 1000 U/ml IFN-α2a, NC is the value of RLU after incubation with the negative control, and S_n is the value of RLU after incubation with samples [23].

2.6. IFN-α2a-incorporated HA-Tyr hydrogels on inhibiting the proliferation of HAK-1B cells

Five hundred microliters of HAK-1B cell suspension containing 12,000 cells was added into each well of the 24-well plate and incubated for 2 days before treatment. HA-Tyr hydrogels with or without IFN-α2a were prepared as described above. Fifty microliters of the hydrogel was added into each of 24-well insert chamber. After 2 h, the hydrogel-loaded inserts were placed into the wells plated with HAK-1B cells, and an additional 500 μl of culture media was added into the insert. The whole plate was incubated for 4 days. Cell viability was assessed using alamarBlue assay according to the manufacturer's protocols. The results were expressed as percentage of viability compared with untreated cells.

2.7. Cell apoptosis assay

HA-Tyr hydrogels with 4.2×10^5 IU/ml of IFN-α2a were prepared as described above. Two hundred microliters of gel precursor solutions of HA-Tyr conjugate, IFN-α2a, HRP and H_2O_2 was added to each 35 mm petri dish. After 2 h, 2.5 ml of 125,000 HAK-1B cells in culture media was added to the petri dishes. As a positive control, 200 μl of IFN-α-2a dissolved in PBS (4.2×10^5 IU/ml) was added to the petri dish with plated cells. After 4 days, the cells in each dish were trypsinized, collected and combined with the floating cells in the cell culture media. Alexa Fluor® 488 annexin V/Dead cell apoptosis kit was applied according to the manufacturer's protocol. Stained cells were sorted by flow cytometry, and the fluorescence intensities of Alexa Fluor 488 (above 1.1×10^4) and PI (above 1×10^3) were considered to be annexin V and PI positives, respectively. The results were presented as percentage of viable (annexin V negative and PI negative), apoptotic (annexin V positive and PI negative) and dead (annexin V positive and PI positive) cells.

2.8. Determination of caspase activity

An Image-iT™ live red caspase detection kit was used to detect and evaluate intracellular apoptotic events in HAK-1B cells. HAK-1B cells were plated on a glass-bottom microwell dish (MatTek Corporation, MA, USA) and treated with HA-Tyr hydrogels that incorporated 4.2×10^5 IU/ml of IFN-α-2a for 4 days. Then cells were stained with fluorescent labeled inhibitor of caspase (FLICA) and Hoechst 33342 according to protocols from Invitrogen. Confocal images were acquired with confocal laser scanning microscopy (Zeiss LSM 5 DUO).

An Apo-ONE® Homogeneous Caspase-3/7 kit was utilized to quantitatively measure caspase-3/7 activity in HAK-1B cells. After cells were treated with IFN-α2a-incorporated HA-Tyr hydrogels for 4 days, cells were lysed with a radio immunoprecipitation assay (RIPA) buffer (Cell Signaling, USA), followed by caspase-3/7 and BCA assay according to protocols from the manufacturers. The caspase-3/7 activity of each sample (FI/μg) was expressed as fluorescence intensity normalized by the protein amount.

2.9. Pharmacokinetics

A mixture of 1.75 wt.% of HA-Tyr solution in PBS containing 0.125 unit/ml HRP, 6×10^7 IU/ml IFN-α2a and different H_2O_2 concentrations (473 μM for HA-Tyr-soft-IFN gel or 728 μM for HA-Tyr-stiff-gel) was subcutaneously injected to the back of 6-week-old female BALB/c nude mice (Biological Resource Center, Biopolis, Singapore) based on the weight of mice (200 μl for each weight of 20 gram). PBS solution containing same amount of IFN-α2a was also injected as a control. Three groups of mice ($n=4$) were treated with HA-Tyr-soft-IFN, HA-Tyr-stiff-IFN and IFN-α2a solution, respectively. At 1, 2, 4, 8 and 24 h after the injection, 20 μl of blood was taken from the tail vein of each mouse. The blood samples were mixed with 3 μl of sodium citrate (37 mg/ml) to prevent blood coagulation, and then were centrifuged at 4 °C, 3,000 g for 5 min. The supernatant of each sample was then taken and stored at −20 °C before measurement. The quantity of human IFN-α2a in the plasma of the mice was then determined by a VeriKine™ Human Interferon-Alpha ELISA kit.

2.10. Tumor regression and delivery of IFN-α2a at tumor site

Two hundred microliters of HAK-1B cells (5×10^7 cells/ml) were subcutaneously injected to the backs of 6-week-old female BALB/c nude mice. Seven days later when diameter of the tumor reached 5–10 mm, the mice were divided into 4 groups ($n=7$) so that the average tumor size in each group was similar. Each mouse received a subcutaneous injection of 100 μl of mixture solution of HA-Tyr conjugate (1.75 wt.%), HRP (0.124 units/ml), H_2O_2 (473 or 728 μM) and IFN-α2a (1.4×10^8 IU/kg) once a week for 2 weeks. Also, a subcutaneous injection of PBS and IFN-α2a dissolved in PBS was performed once a week for 2 weeks as a comparison. Tumors were measured with a digital caliper, and the tumor volumes (mm^3) were calculated from the formula: volume = (length × width^2)/2. On day 20, the mice were sacrificed, and the tumors were then resected and fixed in 4% formalin solution.

To quantify the delivered amount of IFN-α2a at the tumor site, three groups of mice ($n=4$) bearing HAK-1B inoculated tumors with similar size were treated with HA-Tyr-soft-IFN, HA-Tyr-stiff-IFN and IFN-α2a solution, respectively. After 8 h of treatment, the mice were sacrificed and the tumor tissues were resected. Homogenization of tissue was performed and the supernatant of tissue lysate was taken and stored at −20 °C. The quantity of IFN-α2a was determined by a VeriKine™ Human Interferon-Alpha ELISA kit. The care and use of laboratory animals were performed according to the approved protocols by the Institutional Animal Care and Use Committee (IACUC) at the Biological Resource Center (BRC) in Biopolis, Singapore.

2.11. Histology and immunohistochemistry

Tumor tissues were fixed in 4% formaldehyde and embedded in paraffin wax for hematoxylin and eosin staining. Primary and secondary antibodies for TUNEL (Millipore, Singapore) were used for terminal deoxynucleotidyl transferase dUTP nick end labeling (TUNEL) staining. Primary antibody mouse anti-Ki67 NCL-Ki67-MM1 (NOVOcastra, UK) and secondary antibody anti-mouse HRP conjugate (NOVOcastra, UK) were used for Ki67 immunohistochemistry staining. Primary antibody rat anti-CD34 sc-18917 (Santa Cruz, US) and secondary antibody anti-rat HRP conjugate (Santa Cruz, US) were used for CD34 immunohistochemistry staining.

2.12. Statistical analysis

Data from *in vitro* studies are expressed as mean ± standard deviation. Data in animal studies are expressed as mean ± standard error of the mean (SEM). Differences between the values were assessed using one-way ANOVA and Student's *t* test, while $P<0.05$ was considered statistically significant.

3. Results and discussion

3.1. Characterization of IFN-α2a-incorporated HA-Tyr hydrogel

Previously, we reported an injectable hydrogel system composed of hyaluronic acid-tyramine (HA-Tyr) conjugates whose stiffness and gelation rate could be tuned independently by altering the concentrations

of hydrogen peroxide (H_2O_2) and horseradish peroxidase (HRP), respectively [13]. In this study, the HRP concentration was optimized to be at 0.124 units/ml with a gel point around 120 s, in order that the solution of hydrogel precursors would be injectable during the time interval and any uncontrolled diffusion of IFN-α2a after the injection could be avoided or minimized *in situ*. The storage modulus (G') of HA-Tyr hydrogels was 990 Pa and 3078 Pa when the H_2O_2 concentrations were 437 and 728 μM, respectively (Table 1). The significant difference in G' indicated that the stiffness of hydrogels could be tuned with H_2O_2 concentrations. IFN-α2a-incorporated HA-Tyr hydrogels were prepared and characterized in a similar manner. No significant differences were observed in G' between IFN-α2a-incorporated hydrogels and their counterparts without IFN-α2a, which indicates the IFN-α2a incorporation did not interfere with gel formation.

The crosslinking density and mesh size (ε) of the hydrogels were determined based on the measurements of the swelling ratio of hydrogels (Table 1). The crosslinking density of HA-Tyr-soft-IFN was lower than that of HA-Tyr-stiff-IFN while the mesh size of HA-Tyr-soft-IFN gel was significantly larger than that of HA-Tyr-stiff-IFN. Importantly, there was no significance in crosslinking density and mesh size of hydrogels with and without IFN-α2a, which further proved that the incorporation of the protein drug had very minimal effects on the hydrogel formation.

3.2. Release profiles of IFN-α2a from HA-Tyr hydrogels

The concentration of intact IFN-α2a released from hydrogels was determined by ELISA. We observed an initial rapid release of IFN-α2a from HA-Tyr hydrogels (Fig. 1). This rapid release was considered to be due to the protein's concentration difference across the interior of the hydrogel and its external environment [16]. As shown in Table 1, the mesh sizes of HA-Tyr-soft-IFN and HA-Tyr-stiff-IFN were 577 and 407 nm, respectively. As the hydrodynamic radius of IFN-α2a was 2.73 nm [26], and the mesh sizes of the HA-Tyr hydrogels were larger in two orders, that suggests IFN-α2a would diffuse freely within the gel matrix. Indeed, a linear plot was obtained by plotting release of IFN-α2a during the first 8 h as a function of the square root of time, which indicated a typical Fickian diffusion with first order release kinetics (Fig. 1 inset) [14]. The cumulative releases of IFN-α2a from HA-Tyr-soft-IFN and HA-Tyr-stiff-IFN after 8 h reached a plateau and were 78.5 ± 1.4% and 46.0 ± 1.7%, respectively (Fig. 1). In a separate study, freshly prepared HA-Tyr-IFN hydrogels were completely degraded by hyaluronidase *in vitro*. Then, we measured the concentration of IFN-α2a by ELISA. We found that 80.1 ± 0.8% and 56.0 ± 10.6% of IFN-α2a were retrieved from HA-Tyr-soft-IFN and HA-Tyr-stiff-IFN, respectively. These results indicate that the incomplete drug release from HA-Tyr hydrogels was considered to be due to the denaturation of IFN-α2a during crosslinking reaction. In addition, the results suggest that almost all the intact IFN-α2a could be released from HA-Tyr hydrogels by diffusion mechanism without the degradation of hydrogels.

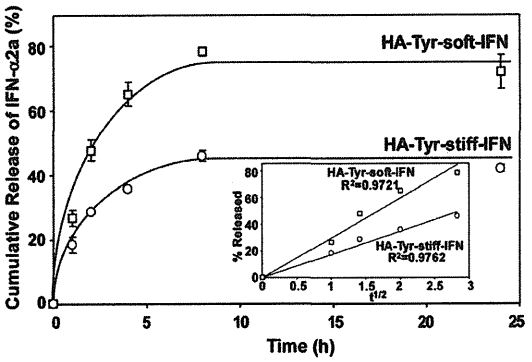

Fig. 1. Cumulative release of IFN-α2a from HA-Tyr-IFN hydrogels ($n = 3$, mean ± standard deviation). The inset shows the cumulative release of protein as a function of the square root of time.

3.3. Effects of crosslinking reaction on the activity of IFN-α2a incorporated in HA-Tyr hydrogels

The activity of IFN-α2a incorporated in the HA-Tyr hydrogel was investigated by an anti-viral assay in Huh-7 cells containing subgenomic Hepatitis C virus (HCV) replicon I_{389}luc-ubi-neo/NS3-3/5.1 [23]. When 2 pg/ml IFN-α2a was used, we found that the inhibition percentages of the viral RNA replication of the IFN-α2a retrieved from PBS, HA-Tyr-soft-IFN and HA-Tyr-stiff-IFN were 29 ± 3, 25 ± 2 and 12 ± 0.4, respectively (Fig. 2). The difference of inhibition percentages between IFN-α2a alone and HA-Tyr-soft-IFN was not statistically significant ($P = 0.11$), indicating the activity of IFN-α2a was well-maintained in HA-Tyr-soft-IFN. In contrast, IFN-α2a retrieved from HA-Tyr-stiff-IFN showed significantly lower activity compared to IFN-α2a solution. The results were further confirmed by using a different dose of IFN-α2a (4 pg/ml). These results clearly demonstrate that it is critical to choose the proper concentration of hydrogen peroxide utilized in the gelation to preserve the activity of the protein in the hydrogel. For HA-Tyr-soft-IFN, a high activity of IFN-α2a was maintained.

3.4. Inhibition of HAK-1B cell proliferation and induction of apoptosis upon treatment with IFN-incorporated HA-Tyr hydrogels

The HAK-1B cell line was established from a single nodule of hepatocellular carcinoma and has been confirmed to retain the morphological and functional characteristics of the original tumor [22]. As shown in Fig. 3a, the viability of HAK-1B was greater than 90% when HA-Tyr hydrogels without IFN-α2a were utilized, indicating the hydrogels are non-cytotoxic. We observed that the percentages of viable cells after treatment with IFN-α2a solution, HA-Tyr-soft-IFN and HA-Tyr-stiff-IFN were 25, 42 and 59, respectively. As we have confirmed the activity of IFN-α2a in HA-Tyr-soft-IFN was similar to that of IFN-α2a solution

Table 1
Characterization of IFN-α2a-incorporated HA-Tyr hydrogels[a].

Sample	H_2O_2 (μM)	G' (Pa)	Q_M	Q_V	ν_e (10^{-6} mol/cm^3)	ε (nm)
HA-Tyr-soft	437	990 ± 49	46.1 ± 0.5	56.4 ± 0.7	1.8 ± 0.04	546.8 ± 7.6
HA-Tyr-soft-IFN	437	898 ± 122[b]	48.3 ± 2.5	59.1 ± 3.0	1.7 ± 0.1[c]	576.8 ± 34.6[d]
HA-Tyr-stiff	728	3078 ± 184	39.3 ± 1.5	48.1 ± 1.9	2.4 ± 0.2	453.2 ± 20.7
HA-Tyr-stiff-IFN	728	3028 ± 199[b]	35.8 ± 2.3	43.8 ± 2.8	2.8 ± 0.3[c]	406.5 ± 30.5[d]

Note. Results are shown as the mean values ± standard deviation ($n = 3$). Abbreviations: storage modulus (G'), mass swelling ratio (Q_M), volumetric swelling ratio (Q_V), effective crosslink density (ν_e), mesh size (ε).

[a] All hydrogels were formed with 1.75 wt.% of HA-Tyr conjugate and 0.124 units/ml of HRP with or without 2.5×10^5 IU/ml of IFN-α2a.

[b] G', [c]ν_e and [d]ε of HA-Tyr hydrogels with IFN-α2a were not significantly different from those of HA-Tyr hydrogels without IFN-α2a ($P > 0.05$).

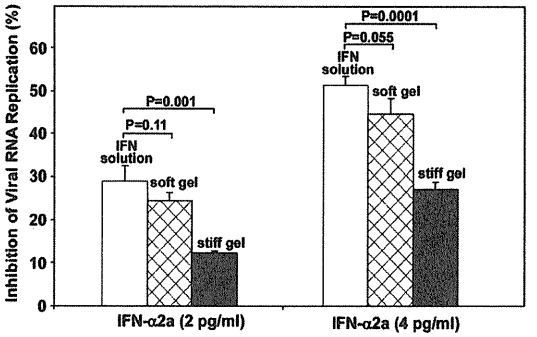

Fig. 2. Anti-viral activity of IFN-α2a retrieved from HA-Tyr-IFN hydrogels after treatment with 250 U/ml hyaluronidase ($n=3$, mean ± standard deviation).

(Section 3.3), the significant difference in cell viability between IFN-α2a solution and HA-Tyr-soft-IFN would be attributed to the prolonged release of IFN-α2a from hydrogels in cell culture.

After treatment with the IFN-α2a or IFN-α2a-incorporated hydrogels, the percentages of live cells dropped significantly as compared to the control (Fig. 3b). On the other hand, the percentages of apoptotic and dead cells increased after treatment with IFN-α2a or IFN-α2a-incorporated hydrogels. The percentages of apoptotic cells treated with IFN-α2a or HA-Tyr-soft-IFN were significantly higher than that of HA-Tyr-stiff-IFN (Table 2). Meanwhile there was no significantly different percentage of apoptotic cells between groups treated by IFN-α2a and HA-Tyr-soft-IFN. These results indicated that HAK-1B cells were undergoing apoptosis after treatment with IFN-α2a-incorporated hydrogels and further confirmed that the activity of IFN-α2a was well-maintained in HA-Tyr-soft-IFN.

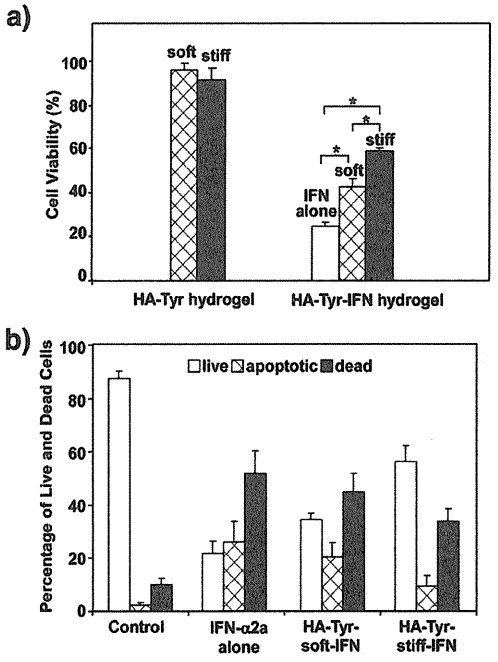

Fig. 3. (a) The viability of HAK-1B cells measured by alarmarBlue assay after 4-day treatment of HA-Tyr hydrogels with or without 4×10^5 IU/ml of IFN-α2a. *: $P<0.05$. (b) Ratio of live/apoptotic/dead HAK-1B cells after treatment of HA-Tyr hydrogels with IFN-α2a (4×10^5 IU/ml) ($n=3$, mean ± standard deviation).

3.5. Caspase-3/7 activity of HAK-1B cells upon treatment with IFN-incorporated HA-Tyr hydrogels

We examined the intracellular activity of caspase-3/7 to investigate the mechanism of apoptosis in HAK-1B after hydrogel treatment. After treatment with IFN-α2a or IFN-α2a-incorporated HA-Tyr hydrogels, the HAK-1B cells showed red fluorescence for active caspase-3/7, whereas cells without treatment showed little staining (Fig. 4a). HA-Tyr-soft-IFN-treated cells showed stronger staining of caspase-3/7 than the HA-Tyr-stiff-IFN-treated cells. Furthermore, the co-staining of caspase-3/7 with cell nuclei in cells treated with the IFN-α2a solution or HA-Tyr-soft-IFN, indicated that those cells were in late stage apoptosis as caspase-3/7 would translocate into nuclear after proteolytic activation and substrate recognition [27]. On the other hand, most of caspase-3/7 stains in HA-Tyr-stiff-IFN-treated cells remained in cytoplasm, indicating an early stage of apoptosis in these cells.

We utilized the Apo-ONE capspase-3/7 assay kit to quantify caspase-3/7 activity in HAK-1B cells after treatment. As shown in Fig. 4b, cells without any treatment showed low fluorescence intensity that indicated there was minimal amount of active caspase-3/7 in the healthy cells. HA-Tyr-soft-IFN-treated cells showed lower fluorescence intensity than IFN-α2a-solution-treated cells, due to the slow release of IFN-α2a from the hydrogel in culture media. On the other hand, HA-Tyr-stiff-IFN-treated cells showed less than half of the fluorescence intensity of HA-Tyr-soft-IFN-treated cells. Such a sizably lower fluorescence intensity is considered to be due to the decreased activity and slower release rate of IFN-α2a from HA-Tyr-stiff-IFN. These results were consistent with the confocal images, and demonstrated that the released IFN-α2a from HA-Tyr hydrogels activated caspase-3/7 in HAK-1B cells.

3.6. Pharmacokinetics of IFN-α2a in the plasma and delivered IFN-α2a in the tumor of mice

We performed the pharmacokinetics study of circulating IFN-α2a in the plasma of mice. As shown in Fig. 5a, at 1 h post injection the concentration of IFN-α2a in the plasma of mice treated with IFN-α2a solution, HA-Tyr-soft-IFN and HA-Tyr-stiff-IFN was 105, 35 and 47 ng/ml, respectively. The high concentration IFN-α2a in the plasma of IFN-α2a-solution-treated mice suggested that the subcutaneously injected IFN-α2a got into the circulation rapidly. In contrast, the concentration of IFN-α2a in the plasma of hydrogel-treated mice was much lower than that of IFN-α2a solution, that indicated a slow release of the protein from the hydrogels at 1 h. From 1 h to 4 h, the concentration of IFN-α2a in the plasma of IFN-α2a solution-treated mice decreased rather rapidly (2 h: 65 ng/ml, 4 h: 8 ng/ml). In contrast, the hydrogel-treated mice plasma showed much slower decreases of IFN-α2a concentrations (HA-Tyr-soft-IFN: 2 h at 30 ng/ml, 4 h at 26 ng/ml; HA-Tyr-stiff-IFN: 2 h at 32 ng/ml, 4 h at 17 ng/ml), that suggested there was a continuous release of IFN-α2a from both types of hydrogels. At 8 h, the concentration of IFN-α2a became negligible in IFN-solution-treated mice, whereas the protein concentration was 8 ng/ml for hydrogel-treated mice. These results clearly

Table 2
Statistical analysis of percentages of live/apoptotic/dead cells upon treatment with IFN-α2a-incorporated HA-Tyr hydrogels[a].

ANOVA test	Live	Apoptotic	Dead
Control vs. HA-Tyr-soft-IFN	**	**	**
Control vs. HA-Tyr-stiff-IFN	**	*	**
IFN-α2a vs. HA-Tyr-soft-IFN	**		
IFN-α2a vs. HA-Tyr-stiff-IFN	**	*	*
HA-Tyr-soft-IFN vs. HA-Tyr-stiff-IFN	**	*	

[a] Statistical analysis was performed using one-way ANOVA and Student's t test.
* $P<0.05$.
** $P<0.01$.

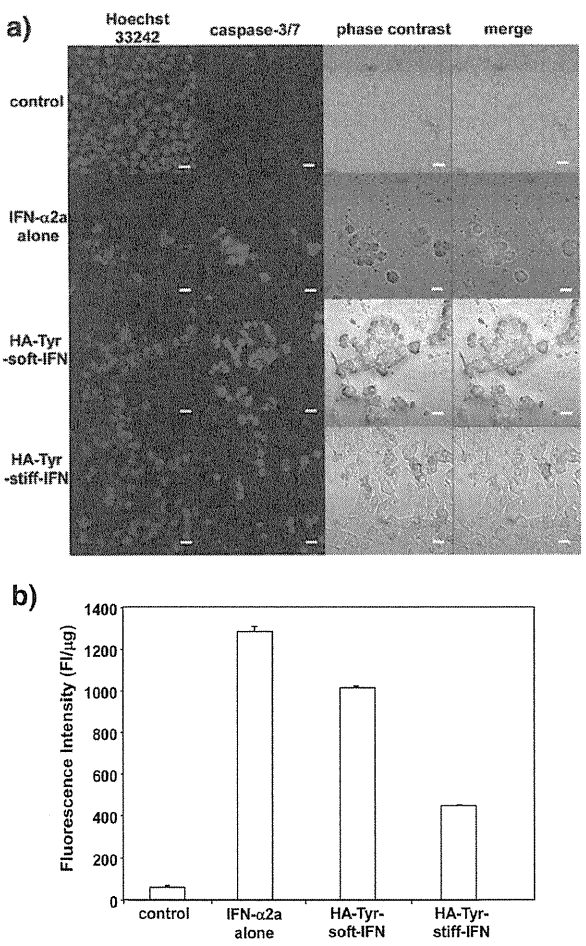

Fig. 4. (a) Confocal images of HAK-1B cells after treatment of HA-Tyr-IFN hydrogels. Cells were stained with Hoechst 33342 (blue) and SR-DEVD-FMK FLICA (red) and pictures were taken with a confocal machine Zeiss LSM 5 DUO. (b) Quantitative measurement of caspase 3/7 activity in cells treated with HA-Tyr-IFN hydrogels. Cells were harvested after treatment and Promega Apo-ONE Homogeneous caspase-3/7 assay as well as BCA protein assay was performed. The results were presented as fluorescence intensity (FI) normalized with the total protein amount (μg) in each sample ($n=3$, mean ± standard deviation). (For interpretation of the references to color in this figure legend, the reader is referred to the web version of the article.)

demonstrated prolonged and continuous release of IFN-α2a from HA-Tyr hydrogels *in vivo*.

Next, we examined the amount of IFN-α2a that was delivered at the tumor site. At 8 h post injection, the delivered amount of IFN-α2a at the tumor site of HA-Tyr-soft-IFN-treated mice was around 1200 pg per gram of tumor tissue, that was three-fold the amount for the IFN-α2a-solution-treated mice (Fig. 5b). The delivered amount of IFN-α2a in HA-Tyr-stiff-IFN-treated mice was two-fold to the delivery for IFN-α2a solution-treated mice. Overall, the IFN-α2a-incorporated hydrogels showed enhanced delivery of the protein drug at the tumor site when compared to protein solution injection.

3.7. Anticancer effect in tumor-xenografted nude mice

The anticancer effect of IFN-α2a-incorporated HA-Tyr hydrogels was examined *in vivo* using a HAK-1B-xenografted nude mouse model. Each group of mice ($n=7$) received subcutaneous injections of HA-Tyr-IFN or IFN-α2a solution. PBS and hydrogels without IFN-α2a were also injected as controls. Fig. 6a shows that the treatment of HA-Tyr hydrogels without

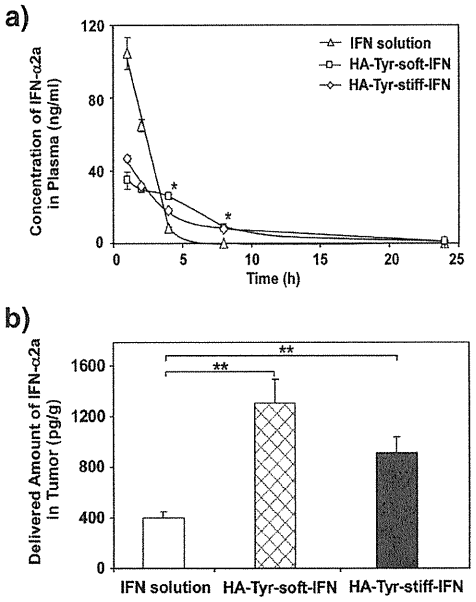

Fig. 5. (a) Pharmacokinetics of IFN-α2a in the plasma of Balb/c nude mice ($n=3$, mean ± standard error of the mean). *: $P<0.05$. (b) Amount of IFN-α2a delivered to tumor tissues of HAK-1B inoculated Balb/c nude mice. The amount of IFN-α2a (pg) delivered at the tumor tissue was normalized with the weight of the tumor (g) ($n=4$, mean ± standard error of the mean). **: $P<0.01$.

IFN-α2a showed no significant effect in tumor regression, that indicates the hydrogel itself has no anti-tumor efficacy. The treatment with IFN-α2a solution did not prevent the growth of tumors as average tumor size in the IFN-α2a solution group was not significantly different

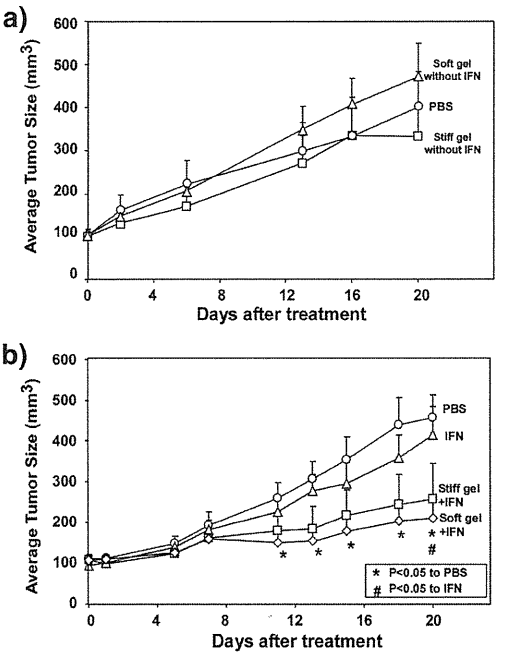

Fig. 6. (a) Tumor regression study of HAK-1B inoculated Balb/c nude mice treated with PBS or HA-Tyr hydrogels without IFN-α2a. (b) Tumor regression study of HAK-1B inoculated Balb/c nude mice treated with PBS, IFN-α2a solution or HA-Tyr-IFN hydrogels ($n=7$, mean ± standard error of the mean).

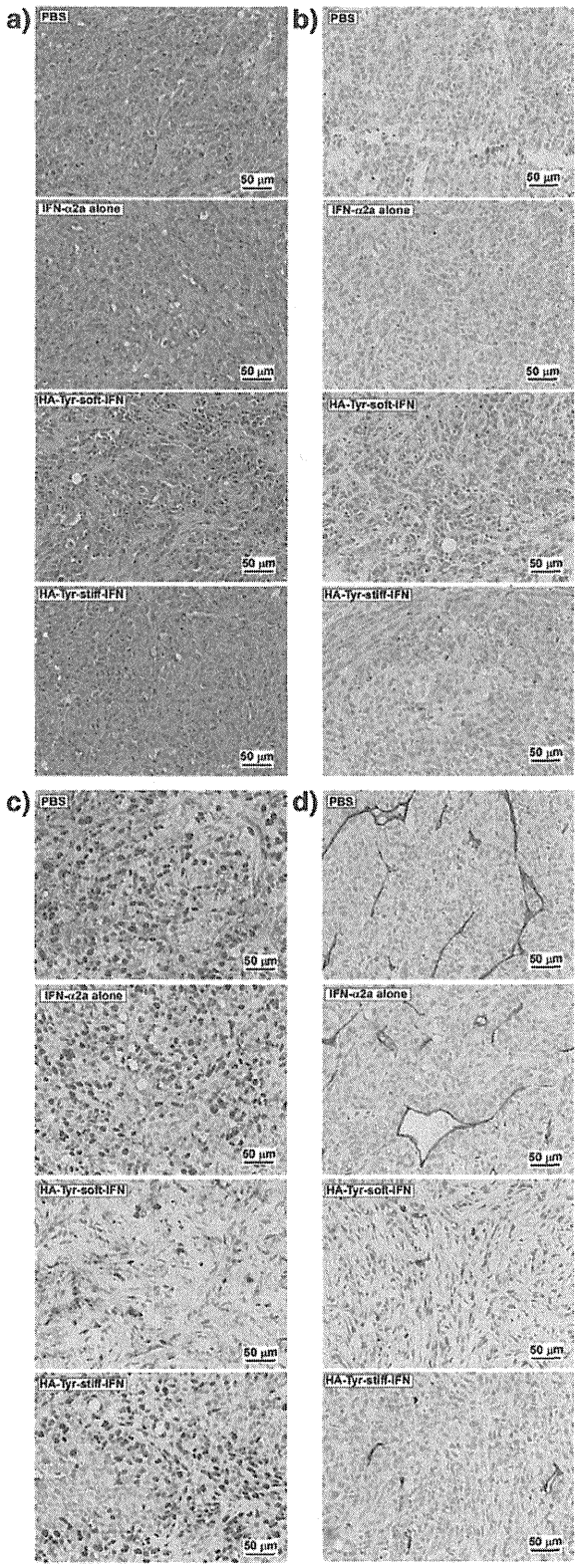

from the PBS group in 20 days (Fig. 6b). In contrast, the groups treated with IFN-α2a-incorporated HA-Tyr hydrogels showed a remarkable decrease in average tumor size. In the group of HA-Tyr-soft-IFN-treated mice, the average tumor size was significantly lower than that of PBS control from day 11 onward ($P<0.05$), that suggested the delivered IFN-α2a from HA-Tyr-soft-IFN effectively inhibited the growth of tumors in mice. We also observed a similar trend of decreasing tumor size in HA-Tyr-stiff-IFN-treated mice, although there was no significant difference in the average tumor size between these mice and PBS control. Thus, IFN-α2a-incorporated HA-Tyr hydrogels have enhanced anti-tumor efficacy in the tumor regression study. In addition, there were minimal side-effects caused by the injection of HA-Tyr hydrogels, as the hydrogel-treated mice maintained their weight and no dead mice were found during the period of study. Also, we did not observe any dead mice from the group without hydrogel-treatment.

We further investigated the histological changes of tumor tissues for the mice treated with IFN-α2a-incorporated hydrogels. Fig. 7a shows the hematoxylin and eosin (H & E) staining of tumor sections from the mice that were treated with PBS, IFN-α2a alone or IFN-α2a-incorporated hydrogels. The nuclei density of tumor cells in HA-Tyr-soft-IFN-treated mice was lower than that of other groups, which was consistent with the results from tumor regression, and confirmed that the treatment with HA-Tyr-soft-IFN showed high antitumor efficacy. Then, we examined the intracellular markers of apoptosis and proliferation in the tumor sections of hydrogel-treated mice. Terminal deoxynucleotidyl transferase dUTP nick end labeling (TUNEL) staining showed a high ratio of apoptotic cells in tumor sections of mice that were treated with HA-Tyr-soft-IFN and HA-Tyr-stiff-IFN (Fig. 7b), that indicated more tumor cells were undergoing apoptosis after treatment with the IFN-α2a-incorporated hydrogels when compared to tumor cells from the PBS group or IFN-α2a solution group. Ki 67 staining revealed an obvious decrease of positive cells in tumor sections in hydrogel-treated mice as compared to the control (Fig. 7c). Since Ki67 is a nuclear protein associated with cellular proliferation [28], it indicated that the tumor cells in HA-Tyr-soft-IFN-treated mice had stopped proliferation and were under senescence. From these results, we summarized that tumor cells were apoptotic and less proliferative in HA-Tyr-soft-IFN-treated mice, while tumor cells were highly proliferative in IFN-α2a-solution-treated mice.

Antiangiogenesis therapy is one of the most significant advances in cancer research [29]. As IFN has been reported to show antiangiogenesis effects in hepatocellular carcinoma [30], we proceeded to examine the angiogenesis of tumor sections of mice after treatment with IFN-α2a-incorporated hydrogels through staining with CD34, which is a cell surface glycoprotein that has been reported as a marker for angiogenesis in cancer [31]. Fig. 7d shows the CD34 staining in the tumor sections of mice that were treated with PBS, IFN-α2a solution or IFN-incorporated hydrogels. In the tumor sections of mice that were treated with PBS or IFN-α2a solution, we observed the positive staining of CD34 with linear, semicircular and circular patterns, indicating an extensive distribution of blood vessels in those samples. In contrast, we only found a few CD34 stains in tumor sections of mice that were treated with IFN-α2a-incorporated hydrogels. This result suggested that angiogenesis was efficiently inhibited in mice that were treated with IFN-incorporated hydrogels.

4. Conclusion

We have demonstrated an injectable IFN-α2a-incorporated HA-Tyr hydrogel system for liver cancer therapy. IFN-α2a-incorporated HA-Tyr hydrogels with tunable stiffness and rapid gelation rate were

Fig. 7. Histological examinations of tumor tissues from HAK-1B inoculated Balb/c nude mice. (a) H & E, (b) TUNEL (brown), (c) Ki67 (brown) and (d) CD34 (brown). (For interpretation of the references to color in this figure legend, the reader is referred to the web version of the article.)

prepared using an enzyme-mediated oxidative coupling reaction involving the Tyr moiety of the HA-Tyr conjugate. The incorporation of IFN-α2a did not change the gelation properties of the hydrogels; the activity of the incorporated protein was well-maintained when a lower concentration of H_2O_2 (437 μM) was used. The release of IFN-α2a from the hydrogels was shown to occur by diffusion *in vitro*. IFN-α2a released from the hydrogels inhibited the proliferation of HAK-1B liver cancer cells, and induced apoptosis through caspase-3/7 pathway. *In vivo* studies revealed that treatment of IFN-α2a-incorporated hydrogels showed improved pharmacokinetics in the plasma of mice, and up to three-fold of IFN-α2a was delivered at the tumor site compared to delivery via IFN-α2a solution injection. In the tumor regression study, treatment with the HA-Tyr-soft-IFN hydrogel reduced the average tumor size significantly from day 11 onwards, while injection with IFN-α2a alone failed to provide antitumor efficacy. Furthermore, histological and immunohistochemical analyses showed lower cell density in tumors after treatment with HA-Tyr-soft-IFN hydrogel, with more apoptotic cells and less proliferating cells as compared to tumors in animals treated with PBS or IFN solution. In addition, angiogenesis was efficiently inhibited in tumors that were treated with IFN-α2a-incorporated hydrogels. Therefore, we provide an alternative approach to improve the anticancer efficacy of protein drugs in liver cancer therapy by using an injectable hydrogel system that incorporates protein therapeutics. We believe that such an approach could be applied to other protein drugs for the treatment of various diseases in the future.

Acknowledgments

This work was supported by the Institute of Bioengineering and Nanotechnology (Biomedical Research Council, Agency for Science, Technology and Research, Singapore). The authors wish to thank JNC Corporation, Japan, for the gift of hyaluronic acid and Prof. Ralf Bartenschlager, University of Heidelberg, Germany, for providing the Huh-7 cells containing subgenomic HCV replicon I_{389}luc-ubi-neo/NS3-3/5.1 with adaptive mutation.

References

[1] G. Walsh, Biopharmaceutical benchmarks 2010, Nat. Biotechnol. 28 (2010) 917–924.
[2] B. Leader, Q.J. Baca, D.E. Golan, Protein therapeutics: a summary and pharmacological classification, Nat. Rev. Drug Discov. 7 (2008) 21–39.
[3] A.C. Chan, P.J. Carter, Therapeutic antibodies for autoimmunity and inflammation, Nat. Rev. Immunol. 10 (2010) 301–316.
[4] L.M. Weiner, R. Surana, S. Wang, Monoclonal antibodies: versatile platforms for cancer immunotherapy, Nat. Rev. Immunol. 10 (2010) 317–327.
[5] N. Lonberg, Fully human antibodies from transgenic mouse and phage display platforms, Curr. Opin. Immunol. 20 (2008) 450–459.
[6] R.E. Kontermann, Strategies for extended serum half-life of protein therapeutics, Curr. Opin. Biotechnol. 22 (2011) 868–876.
[7] W.H. Vogel, Infusion reactions: diagnosis, assessment, and management, Clin. J. Oncol. Nurs. 14 (2010) E10–E21.
[8] A.S. Hoffman, Hydrogels for biomedical applications, Adv. Drug Deliv. Rev. 54 (2002) 3–12.
[9] L.S. Wang, J.E. Chung, P.P.Y. Chan, M. Kurisawa, Injectable biodegradable hydrogels with tunable mechanical properties for the stimulation of neurogenesic differentiation of human mesenchymal stem cells in 3D culture, Biomaterials 31 (2010) 1148–1157.
[10] W.S. Toh, T.C. Lim, M. Kurisawa, M. Spector, Modulation of mesenchymal stem cell chondrogenesis in a tunable hyaluronic acid hydrogel microenvironment, Biomaterials 33 (2012) 3835–3845.
[11] M. Kurisawa, J.E. Chung, Y.Y. Yang, S.J. Gao, H. Uyama, Injectable biodegradable hydrogels composed of hyaluronic acid-tyramine conjugates for drug delivery and tissue engineering, Chem. Commun. 14 (2005) 4312–4314.
[12] M. Kurisawa, F. Lee, L.S. Wang, J.E. Chung, Injectable enzymatically crosslinked hydrogel system with independent tuning of mechanical strength and gelation rate for drug delivery and tissue engineering, J. Mater. Chem. 20 (2010) 5371–5375.
[13] F. Lee, J.E. Chung, M. Kurisawa, An injectable enzymatically crosslinked hyaluronic acid-tyramine hydrogel system with independent tuning of mechanical strength and gelation rate, Soft Matter 4 (2008) 880–887.
[14] F. Lee, J.E. Chung, M. Kurisawa, An injectable hyaluronic acid-tyramine hydrogel system for protein delivery, J. Control. Release 134 (2009) 186–193.
[15] X.Z. Shu, Y.C. Liu, F.S. Palumbo, Y. Lu, G.D. Prestwich, In situ crosslinkable hyaluronan hydrogels for tissue engineering, Biomaterials 25 (2004) 1339–1348.
[16] S. Cai, Y. Liu, X. Zheng Shu, G.D. Prestwich, Injectable glycosaminoglycan hydrogels for controlled release of human basic fibroblast growth factor, Biomaterials 26 (2005) 6054–6067.
[17] C.M. Nimmo, S.C. Owen, M.S. Shoichet, Diels–Alder click cross-linked hyaluronic acid hydrogels for tissue engineering, Biomacromolecules 12 (2011) 824–830.
[18] J.H. Hoofnagle, K.D. Mullen, D.B. Jones, V. Rustgi, A. Dibisceglie, M. Peters, J.G. Waggoner, Y. Park, E.A. Jones, Treatment of chronic non-A, non-B Hepatitis with recombinant human alpha-interferon — a preliminary report, N. Engl. J. Med. 315 (1986) 1575–1578.
[19] A.U. Neumann, N.P. Lam, H. Dahari, D.R. Gretch, T.E. Wiley, T.J. Layden, A.S. Perelson, Hepatitis C viral dynamics in vivo and the antiviral efficacy of interferon-alpha therapy, Science 282 (1998) 103–107.
[20] H. Yano, A. Iemura, M. Haramaki, S. Ogasawara, A. Takayama, J. Akiba, M. Kojiro, Interferon alfa receptor expression and growth inhibition by interferon alfa in human liver cancer cell lines, Hepatology 29 (1999) 1708–1717.
[21] T. Hisaka, H. Yano, S. Ogasawara, S. Momosaki, N. Nishida, Y. Takemoto, S. Kojiro, Y. Katafuchi, M. Kojiro, Interferon-alpha Con1 suppresses proliferation of liver cancer cell lines in vitro and in vivo, J. Hepatol. 41 (2004) 782–789.
[22] H. Yano, A. Iemura, K. Fukuda, A. Mizoguchi, M. Haramaki, M. Kojiro, Establishment of 2 distint human hepatocellular carcinoma cell lines from a single nodule showing clonal dedifferentiation of cancer cells, Hepatology 18 (1993) 320–327.
[23] J.M. Vrolijk, A. Kaul, B.E. Hansen, V. Lohmann, B.L. Haagmans, S.W. Schalm, R. Bartenschlager, A replicon-based bioassay for the measurement of interferons in patients with chronic hepatitis C, J. Virol. Methods 110 (2003) 201–209.
[24] T. Pietschmann, M. Zayas, P. Meuleman, G. Long, N. Appel, G. Koutsoudakis, S. Kallis, G. Leroux-Roels, V. Lohmann, R. Bartenschlager, Production of infectious genotype 1b virus particles in cell culture and impairment by replication enhancing mutations, PLoS Pathog. 5 (2009) 14.
[25] J.B. Leach, K.A. Bivens, C.W. Patrick, C.E. Schmidt, Photocrosslinked hyaluronic acid hydrogels: natural, biodegradable tissue engineering scaffolds, Biotechnol. Bioeng. 82 (2003) 578–589.
[26] C. Dhalluin, A. Ross, L.A. Leuthold, S. Foser, B. Gsell, F. Muller, H. Senn, Structural and biophysical characterization of the 40 kDa PEG-interferon-alpha2a and its individual positional isomers, Bioconjug. Chem. 16 (2005) 504–517.
[27] S. Kamada, U. Kikkawa, Y. Tsujimoto, T. Hunter, Nuclear translocation of caspase-3 is dependent on its proteolytic activation and recognition of a substrate-like protein(s), J. Biol. Chem. 280 (2005) 857–860.
[28] J. Bullwinkel, B. Baron-Luhr, A. Ludemann, C. Wohlenberg, J. Gerdes, T. Scholzen, Ki-67 protein is associated with ribosomal RNA transcription in quiescent and proliferating cells, J. Cell. Physiol. 206 (2006) 624–635.
[29] N. Ferrara, R.S. Kerbel, Angiogenesis as a therapeutic target, Nature 438 (2005) 967–974.
[30] D. Ribatti, A. Vacca, B. Nico, D. Sansonno, F. Dammacco, Angiogenesis and anti-angiogenesis in hepatocellular carcinoma, Cancer Treat. Rev. 32 (2006) 437–444.
[31] M.-C. Bettencourt, J.J. Bauer, I.A. Sesterhenn, R.R. Connelly, J.W. Moul, CD34 immunohistochemical assessment of angiogenesis as a prognostic marker for prostate cancer recurrence after radical prostatectomy, J. Urol. 160 (1998) 459–465.

Article type: Original Article - Hepatology (Experimental)

Received date: 04-Apr-2013

Accepted date: 15-Nov-2013

Title: SP cell fractions from HCC cell lines increased with tumor dedifferentiation, but lack characteristic features of CSCs.

Masamichi Nakayama[1)2)], Sachiko Ogasawara[1)], Jun Akiba[1)], Kousuke Ueda[1)], Keiko Koura[1)2)], Keita Todoroki[1)], Hisafumi Kinoshita[2)], Hirohisa Yano[1)]

1) Department of Pathology, Kurume University School of Medicine, Kurume, Japan

2) Department of Surgery, Kurume University School of Medicine, Kurume, Japan

Corresponding author: Jun Akiba

Address: Department of Pathology, Kurume University School of Medicine,

67 Asahimachi, Kurume 830-0011, JAPAN

Tel: +81-942-31-7546

Fax: +81-942-32-0905

E-mail: akiba@med.kurume-u.ac.jp

Abstract

Background and Aim: Cancer stem cells (CSCs), a minority population with stem cell-like characteristics, play important roles in cancer development and progression. Putative CSC markers, such as CD13, CD90, CD133, and EpCAM, and side population (SP) technique are generally used in an attempt to isolate CSCs. We aimed to clarify the relationship between CSCs and clonal dedifferentiation in hepatocellular carcinoma (HCC).

Methods: We used a well-differentiated HCC cell line (HAK-1A) and a poorly differentiated HCC cell line (HAK-1B) established from a single nodule with histological heterogeneity. HAK-1B arose due to clonal dedifferentiation of HAK-1A. The SP cells and non-SP (NSP) cells were isolated from the two cell lines with a FACSAria II and used for the analyses.

Results: The SP cell fractions in HAK-1A and HAK-1B were 0.2% and 0.9%, respectively. CD90 or EpCAM was not expressed in either HAK-1A or HAK-1B, while CD13 and CD133 were expressed in HAK-1B alone. Although sphere forming ability, tumorigenicity, growth rate, and CD13 expression were higher in HAK-1B SP cells than HAK-1B NSP cells, there were no differences in drug resistance, colony forming ability, or cell cycle rates between HAK-1B SP and NSP cells, suggesting HAK-1B SP cells do not fulfill CSC criteria.

Conclusions: Our findings suggested a possible relationship between the expression of CSC markers and clonal dedifferentiation. However, the complete features of CSC could not be identified in SP cells, and the concept of SP cells as a universal marker for CSC may not apply to HAK-1A and HAK-1B.

Keywords: cancer stem cells, side population cells, dedifferentiation

Introduction

Cancer stem cells (CSCs) are defined by self-renewing capacity, differentiation capacity, and tumor-initiating capacity. Additionally, the seeding of metastasis and tumor relapse are attributed to CSCs [1-3]. To date, the existence of CSCs has been proven not only in hematopoietic neoplasms [4, 5], but also various solid neoplasms [6-11].

Side population (SP) cell sorting was initially applied for the identification of hematopoietic stem cells and has been used to enrich stem cell compartments in diverse tissues and organs [12-14]. SP cells are detected by their ability to efflux Hoechst 33342 dye through ATP-binding cassette (ABC) membrane transporters. Recently, SP cells have also been used in an attempt to isolate a stem cell–like fraction in cancer cells [15-17]. The approach seems valuable because a variety of cancers, including HCC, highly express ABC transporters, which are reported to contribute to multi-drug resistance [18].

A variety of markers have been successfully used to enrich CSC fractions from different tumors including HCC [19]. Although no markers for putative liver CSCs have been generally accepted, CD133, CD90, epithelial cell adhesion molecule (EpCAM) and CD13 are thought to be candidates for liver CSC markers [20-24].

Recent evidence suggests that CSCs, a minority population with stem-cell-like characteristics, play important roles in cancer development and progression [25].

In this study, we isolated the SP and non-SP (NSP) cells from two HCC cell lines, a well-differentiated human HCC cell line (HAK-1A) and a poorly differentiated HCC cell line (HAK-1B) which were established from a single nodule with a three-layered structure having different histologic features [26], and compared the relationship between CSCs and clonal dedifferentiation.

Materials and methods

Cell lines and cell culture

This study used two human HCC cell lines: HAK-1A, HAK-1B, which were both established from a single HCC nodule showing a three-layered structure with a different histological grade in each layer [26]. HAK-1A resembles well-differentiated HCC cells in the outer layer of the original tumor, and HAK-1B resembles poorly differentiated cells in the inner layer. The presence of an identical point mutation in the p53 gene in the two cell lines suggests that they are of clonal origin. The cell culture condition is described elsewhere [26].

SP cell analysis using flow cytometry

We followed the protocol previously reported by Goodell et al. [13], with minor modifications. Briefly, cells were detached from the culture dish with Accutase (Innovative Cell Technologies, Inc., San Diego, CA, USA). The cells were incubated at 37 °C for 60 minutes with Hoechst 33342 (SIGMA-Aldrich, Saint Louis, MO, USA). The control cells were incubated in the presence of 15 μg Reserpine (SIGMA-Aldrich). After staining, the cells were suspended in PBS with 2% FBS, filtered through a 40 μm cell strainer (BD Biosciences, San Jose, CA, USA). Cells were counterstained with 0.5 μg/mL propidium iodide (PI, BD Biosciences) for the discrimination of dead cells. Viable cells were analyzed and isolated by a FACSAria II (BD Biosciences).

Immunofluorescence flow cytometric analysis of SP and NSP cells

We analyzed SP and NSP cells isolated from HAK-1A and HAK-1B for expression of the putative stem cell markers CD133, CD90, EpCAM and CD13. Cells were first stained with Hoechst 33342. Excess dye was removed by resuspending 1×10^6 cells/mL in PBS with 2% FBS. Cells were incubated in the dark at 4 °C for 30 minutes with fluorescence-conjugated monoclonal antibodies, including allophycocyanin (APC) -conjugated mouse anti human CD133/2 (293C3) antibodies (Miltenyi Biotec, Bergisch-Gladbach, Germany), fluorescein isothiocyanate (FITC) -conjugated mouse

anti human CD90, phycoerythrin (PE) -conjugated mouse anti human EpCAM and Purified Mouse Anti-Human CD13 (BD Biosciences). After 30 minutes, cells with Purified Mouse Anti-Human CD13 were also incubated in the dark at 4 °C for 30 minutes with Goat Anti-Mouse Ig FITC (BD Biosciences). Cells were counterstained with 0.5 μg/mL PI for the discrimination of dead cells. The data were analyzed using a FACSAria II.

Generation of SP and NSP cells by SP or NSP cells

A total of 1 x 10^5 sorted SP cells or NSP cells from HAK-1A and HAK-1B were cultured for 1 week, and used for SP cell analysis, as described above, to examine whether SP or NSP cells generate SP and NSP cells.

Proliferation of HAK-1B SP and NSP cells

The proliferative ability of the cells from each subpopulation, including HAK-1B SP and NSP cells was examined using colorimetric assays with 3-(4, 5-dimethylthiazol-2yl-yl-)-2, 5-dimethyl tetrazolium bromide (MTT) cell growth assay kits (Chemicon, Temecula, CA, USA), as described elsewhere [27]. SP and NSP cells (1500 cells/well) were seeded on 96-well plates (Falcon, Becton Dickinson Labware, Tokyo, Japan) by a FACS Aria II. After culture for 24 h, 48 h, 72 h, 96 h, or 120 h, the number of viable cells was examined.

Effects of CDDP, 5-FU, and PEG-IFN-α2b on the proliferation of HAK-1B SP and NSP cells

Effects of Cisplatin (CDDP) (Nihonkayaku, Tokyo, Japan), 5-fluorouracil (5-FU) (Kyowa Hakko, Tokyo, Japan) and pegylated IFN-α2b (PEG-IFN-α2b) (Schering-Plough K.K., Osaka, Japan) on cell proliferation were examined by MTT assay. SP and NSP cells (1,500 cells/well) were seeded on 96-well plates, cultured for 24 h, and then the culture

medium was replaced with a new medium containing CDDP alone (0, 0.125, 0.25 or 0.5 μg/mL); 5-FU alone (0, 0.75, 1.5 or 3 μM); or PEG-IFN-α2b (0, 500, 1,000 or 2,000 IU/mL). After culturing for 48 h or 96 h, the number of viable cells was examined by MTT assay.

Drug treatment assay of SP and NSP cells in HAK-1A and HAK-1B

HAK-1A and HAK-1B cells were cultured with medium alone (Control) or medium containing 5-FU (1.5 μM) or PEG-IFN-α2b (1,000 IU/mL) and cultured for 96 hours, and SP cell analysis, as described above, was performed to estimate the effect of drugs on SP cell fraction.

Cell cycle analysis of HAK-1B SP and NSP cells

Cultured HAK-1B cells were labeled with 10mM bromodeoxyuridine (BrdU) (Sigma Chemical Co., St. Louis, MO) for 30 min, harvested, and used for the isolation of SP and NSP by a FACSAria II. Isolated SP or NSP cells were used for cell cycle analysis according to the technique described elsewhere [28]. The percentage of the cells in the G_1, S or G_2/M phase was calculated from a dot plot.

Colony formation assay of HAK-1B SP and NSP cells

Colony formation assay was performed almost according to a modified previously described method [29]. The number of colonies > 0.5 mm in diameter was counted 14 days later.

Sphere formation assay of HAK-1B SP and NSP cells

We performed sphere formation assay according to a previously described method [29].

Tumorigenicity assay of HAK-1B SP and NSP cells *in vivo*

Various numbers of cells (1, 5, 10, 50, or 100 x 10^3) were injected subcutaneously into 4-week-old female NOD/SCID mice (n=5 in each group). Tumorigenic capacity was judged 8 weeks after injection. All procedures were approved by the Ethics Review Committee for Animal Experimentation of Kurume University School of Medicine.

Gene expression microarrays of SP and NSP cells isolated from HAK-1A and HAK-1B

The cRNA was amplified, labeled, and hybridized to a 44K Agilent 60-mer oligomicroarray according to the manufacturer's instructions. All hybridized microarray slides were scanned by an Agilent scanner. Relative hybridization intensities and background hybridization values were calculated using Agilent Feature Extraction Software (9.5.1.1).

Quantitative real-time reverse transcriptase-polymerase chain reaction (qRT-PCR) of SP and NSP cells isolated from HAK-1A and HAK-1B

Total RNA was extracted using RNeasy Plus Micro Kit (Qiagen, Valencia, CA, USA) and complementary DNA (cDNA) was synthesized using Reverse Transcription System (Promega, Madison, WI, USA) according to the manufacturer's instructions. qRT-PCR was carried out with TaqMan technology using ABI PRISM 7500 (Applied Biosystems, Foster City, CA, USA) followed by a previously published method [29]. Gene expression assays primer and probe mixes were used for CD13, CD133, CD24, CD44, CD90, EpCAM, ABCG2, Oct-4, Nanog, BMI1, Alb, CYP3A4 and β-actin (assay IDs are listed in Table 1; Applied Biosystems).

Statistical analysis

Comparison of colorimetric cell growth, drug resistance, colony forming ability and sphere forming ability were performed using Student's *t*-test. Differences were considered significant at $P<0.05$.

Results

1. Identification of SP and NSP cells in HAK-1A and HAK-1B and expression of CSC markers

The SP cell fraction in HAK-1A was very low at only 0.2%. Expression of the putative CSC markers, such as CD133, CD90, EpCAM, CD13, was almost completely absent in both SP and NSP cells from HAK-1A (Fig. 1a). The SP fraction in HAK-1B was 0.9%. Moreover, while CD90 and EpCAM expression was absent in HAK-1B SP and NSP cells, CD133 expression was observed both in 4.6～6.4% of HAK-1B SP cells and in 3.9～5.3% of HAK-1B NSP cells. CD13 expression was higher in SP cells (21.7%) than in NSP cells (8.9%) (Fig. 1b).

2. Generation SP and NSP cells from sorted SP and NSP cells in HAK-1A and HAK-1B

After culturing HAK-1A SP cells or HAK-1B SP cells for 1 week, the percentage of HAK-1A and HAK-1B SP cells decreased to 1.9% and 7.3%, respectively. In contrast, culture of HAK-1A SP cells and HAK-1B NSP cells generated a small population of SP cells in HAK-1A (0.1%) and HAK1B (0.7%). The results suggest the SP cells could generate NSP cells, and vice versa (Fig. 2).

3. Biological features of SP and NSP cells in HAK-1B cells *in vitro*.

In HAK-1B, SP cell growth was significantly higher than that of NSP cells at every time point (24 h, 48 h, 72 h, 96 h, and 120 h; Fig. 3a). The cell cycle analysis revealed no obvious differences in G_0-G_1/ S/ G_2-M ratios between SP cells (64.0%/ 30.1%/ 4.2%) and NSP cells (65.3%/ 31.9%/ 1.6%) (Fig. 3b).

Drug resistance to 5-FU, CDDP or PEG-IFN-α2b was examined. The results showed that the viability of HAK-1B SP cells (58.7%) was significantly lower than that of HAK-1B NSP cells (71.5%) at 96 h in cells treated with 0.75 μM 5-FU (P<0.001).

Similarly, after 96 h treatment with 1.5 μM 5-FU, viability of SP cells fell to 40.7%, compared with 47.9% in NSP cells ($P<0.05$). SP cell viability was also significantly lower (50.7%) than NSP cells (63.5%)($P<0.05$) after 96 h treatment with 500 IU/mL PEG-IFN-α2b. No other significant differences were observed between SP and NSP cells (Fig. 3c). After exposure of HAK-1B cells to PEG-IFN-α2b for 72 h, the percentage of SP cells decreased as compared with control. Conversely, the percentage of SP cells increased when HAK-1B cells were treated with 5-FU for 72 h (Fig. 3d).

In the colony formation assay, SP cells from HAK-1B formed 252 ±33.4 colonies, while the NSP cells formed 243 ±70.1 colonies; this difference was not significant (Fig. 4a). Sphere formation was significantly higher in SP cells (21.0±4.1 spheres) as compared with NSP cells (15.7±2.7 spheres) in the HAK-1B cell line ($P<0.05$; Fig. 4b).

4. Biological features of SP and NSP cells in HAK-1B cells *in vivo*.

Injection of 1, 5, or 10 x 10^3 SP or NSP cells produced no tumors in NOD/SCID mice. In contrast, four mice that received 5 x 10^4 SP cells and five mice that received 10 x 10^4 SP cells developed tumors at 8 weeks. In addition, one mouse that received 5 x 10^4 NSP cells and two mice that received 10 x 10^4 NSP cells also developed small tumors (Fig.4c).

5. cDNA microarray analysis of gene expression in SP and NSP cells sorted from HAK-1A or HAK-1B cells

cDNA microarray analysis found 884 and 470 differences in gene expression between HAK-1A and HAK-1B, respectively, but there were no significant differences between SP and NSP cells in expression of stemness genes (e.g., CD44, Oct-4, Bim-1, ABCG2, CD24, EpCAM)(Table 2).

6. qRT-PCR analysis of SP and NSP cells in HAK-1A or HAK-1B cells

SP and NSP cells of HAK-1A and HAK-1B expressed mRNAs of CSC markers, such as